

Mixed Ligand Complexes with 4-Aminoantipyrine Derivatives to Combat Natural Antioxidant System: Synthesis, Characterization and Biological Studies

J. JOSEPH* and G. AYISHA BIBIN RANI

Department of Chemistry, Noorul Islam Centre for Higher Education, Kumaracoil-629 180, India

*Corresponding author: E-mail: chem_joseph@yahoo.co.in

Received: 23 January 2014;

Accepted: 17 September 2014;

Published online: 19 January 2015;

AJC-16674

Novel 4-aminoantipyrine based mixed ligand metal complexes with the Schiff bases of L¹ (L¹- 4-aminoantipyrine with furfuraldehyde and L²/L³/L⁴/L⁵ are and L²-2-aminophenol with salicylaldehyde, L³-2-aminophenol with cinnamaldehyde, L⁴-2-aminobenzothiazole with salicylaldehyde, L⁵-2-aminobenzothiazole with cinnamaldehyde) were synthesized. The structures of the mixed ligand complexes were established by analytical and spectral techniques. They were screened for *in vitro* antimicrobial activity against of bacteria and fungi by disc diffusion method. The interaction of metal complexes with calf thymus-DNA (CT-DNA) was investigated by UV-visible, cyclic voltammetry, viscosity and thermal denaturation studies. DNA interaction studies suggest that metal complex binds to calf thymus-DNA through intercalation mode. Superoxide dismutase activity of these complexes has also been studied. The free ligands and their metal complexes have been tested for *in vitro* antioxidant activity by the reduction of 1,1-diphenyl-2-picryl hydrazyl (DPPH). The antioxidant activities of the complexes were studied and compared with the activity of ascorbic acid. Copper(II) complex showed superior antioxidant activity than other complexes.

Keywords: 4-Aminoantipyrine, Mixed ligand complex, Viscosity, DNA binding, Antioxidant activity, Antimicrobial activity.

INTRODUCTION

The chemistry of metal complexes with tailor made Schiff base ligands and their application have considerable interest because of their preparative accessibility, diverse reactivity and structural variability. Many drugs involve heterocycles, sulphur, oxygen, nitrogen, amino-nitrogen, azomethine nitrogen and alcoholic or phenolic oxygen are some of the donor atoms of interest. Schiff base complexes incorporating phenolic group as chelating moieties in the ligand are considered as models for executing important biological reactions and mimic the catalytic activities of metalloenzymes¹.

Thiazole derivatives have been found a number uses in medicinal and pharmaceutical fields². Some of them have been showed to have antitumor activity³ anticandidal⁴ parkinson's disease⁵ antihistaminic and anti-inflammatory⁶. 2-Aminobenzothiazole used to biological activity as fungicides, antibiotics, pesticides, herbicides and neuro protectors⁷⁻⁹. Schiff bases of salicylaldehydes have also been reported as plant growth regulators¹⁰ and antimicrobial¹¹ or antimycotic¹² activity. Transition metal complexes containing salicylaldehyde are commonly found in biological media and play important roles in processes such as catalysis of drug interaction with biomolecules¹³. Cinnamaldehyde is an aromatic aldehyde and main component of bark extract of cinnamon¹⁴. The main advantage of cinnamal-

dehyde is that direct contact is not required for being active as antimicrobial. Cinnamaldehyde has been shown to be active against a range of forborne pathogens bacteria¹⁵. Nontoxic doses of cinnamaldehyde and cinnamaldehyde derivatives have previously been reported to potentiate the cell-inactivating effect of *cis*-diamminedichloro platinum(II) in human NHIK 3025 cells in culture¹⁶.

The transition metal complexes of 4-aminoantipyrine and its derivatives have been extensively examined due to their wide applications in various fields like biological, analytical, therapeutical¹⁵⁻¹⁸ antifungal, antibacterial, analgesic, sedative, antipyretic and anti-inflammatory agents¹⁹⁻²³. Antipyrine Schiff base derivatives can also serve as antiparasitic agents and their complexes with platinum(II) and cobalt(II) ions have been shown to act as antitumor substances.

Recently, metal complexes show biological activity in many mammalian cell systems *in vitro* and *in vivo* have been investigated as to their interaction with DNA. Hence, much of the attention has been targeted on the design of metal-based complexes, predominantly Cu(II) complexes, which can bind and cleave DNA. Copper is a bio essential element in all living systems. Recently, numerous research groups have reported novel Cu(II) complexes with organic ligands showing anti-fungal and antibacterial properties against several pathogenic fungi and bacteria^{24,25}.

The superoxide radical anion ($O_2^{\cdot-}$) is an inevitable by-product of aerobic metabolism which if not eliminated may cause significant cellular damage. Consequently, the superoxide radical has been implicated in numerous medical disorders^{26,27}. To avoid such harmful consequences, all oxygen metabolizing organisms possess metalloenzymes, known as superoxide dismutases (SODs). Superoxide dismutases are dedicated to keeping the concentration of $O_2^{\cdot-}$ in controlled low limits, thus protecting biological molecules from oxidative damage. These superoxide dismutases disproportionate the toxic $O_2^{\cdot-}$ radical to molecular oxygen and hydrogen peroxide^{28,29}.

In the present study, we have reported the biochemical, DNA binding and antioxidant studies of mixed-ligand complexes. They were characterized using analytical and spectral techniques.

EXPERIMENTAL

All chemicals used in the present work *viz.*, 4-aminoantipyridine, furfuraldehyde 2-aminophenol, 2-aminobenzothiazole, salicylaldehyde, cinnamaldehyde, Fe(III), Co(II), Cu(II), Ni(II) and Zn(II) chlorides were of analAR (Merck). The solvents were distilled and used for the synthesis of the ligands and metal complexes before use. Calf thymus DNA was purchased from Genie Biolab, Bangalore, India.

The elemental analysis was performed using Elementar Vario EL III Carlo Erba 1108. The amount of metal present in the metal complexes was estimated using ammonium oxalate method³⁰. IR spectra of the Schiff base ligands and their metal complexes were recorded on Perkin-Elmer FT-IR 783 Spectrophotometer in 4000-300 cm^{-1} range using KBr disc. 1H NMR spectra were recorded on a Bruker Avance Dry 300 MHz FT-NMR Spectrometer in DMSO with TMS as the internal reference. DSC Curves were recorded on DSC 910 Modular Coupled to a 2000 thermal analyser. The FAB mass spectrum of the Schiff base ligands and their complexes were recorded on a JEOL SX 102/DA-6000 mass spectrometer/data system using argon/xenon (6 kV, 10 mA) as the FAB gas. ESR spectra of the mixed ligand copper complex was recorded on a Varian E 112 EPR Spectrometer in DMSO solution both at room temperature (300 K) and at liquid nitrogen temperature (77 K) using TCNE (tetracyanoethylene) as the g marker. Electronic absorption spectra of the Schiff base ligands and their mixed ligand complexes were recorded in DMSO using a Systronics 2201 double beam UV-visible, spectrophotometer. Molar conductance of the metal complexes was measured in DMSO solution using a coronation digital conductivity meter. The magnetic susceptibility values were calculated using the relation $\mu_{eff} = 2.83 (\chi_m \cdot T)^{1/2}$. The diamagnetic corrections were made by Pascal's constant and $Hg[Co(SCN)_4]$ was used as a calibrant. Electrochemical experiments were performed on a CHI 604D electrochemical analysis system with a three-electrode system consists a glassy carbon working electrode, Pt wire auxiliary electrode and Ag/AgCl reference electrode. Tetrabutylammoniumperchlorate (TBAP) was used as the supporting electrolyte. All solutions were purged with N_2 for 30 min prior to each set of experiments.

Preparation of ligands: The Schiff base ligands (L^1 , L^2 , L^3 , L^4 , L^5) were prepared according to earlier reports, with slight modifications³¹⁻³³.

L^1 : The Schiff base L^1 was prepared by a dropwise addition, with stirring, of ethanolic solution of furfuraldehyde, to an ethanolic solution of 4-aminoantipyridine, respectively. The reaction mixture was refluxed on a water bath for 1-2 h. On cooling, the solid products were separated and filtered. Schiff bases were recrystallized from ethanol and dried in vacuo over P_4O_{10} , to yield yellow crystals. 1H NMR (DMSO- d_6 , δ , ppm): Phenyl multiplet at 6.9-7.37 δ (m, 5H), -CH=N at 8.1 (furfuryl moiety, s, 1H), -C-CH₃ at 2.4 δ (s, 3H), N-CH₃ at 3.2 δ (s, 3H), furfuryl protons at 6.5-7.7 δ (m, 3H). ^{13}C NMR (DMSO- d_6 , δ , ppm): 34.5 (C₁), 160.1 (C₂), 110.3 (C₃), 150.4 (C₄), 12.8 (C₅), 163.2 (C₆), 148.9 (C₇), 119.1 (C₈), 111.9 (C₉), 144.1 (C₁₀), 123.5 (C₁₁), 128.6 (C₁₂), 121.5 (C₁₃), 129.1 (C₁₄), 123.3 (C₁₅), 133.5 (C₁₆).

L^2 - L^5 : The ligand (L^2 - L^5) was prepared by the condensation of equimolar ratio of 2-aminophenol (L^2 - L^3) with salicylaldehyde/cinnamaldehyde and 2-aminobenzothiazole, (L^4 - L^5) with salicylaldehyde/cinnamaldehyde in ethanolic medium. The resulting reaction mixture was stirred well, refluxed for 3-6 h and then allowed to cool overnight. The coloured solid precipitate of Schiff base obtained was filtered, washed with cold ethanol and dried *in vacuo*.

L^2 : 1H NMR (DMSO- d_6 , δ , ppm): phenyl multiplet at 6.9-7.6 d (m, 8H), -CH=N at 8.8 d (phenyl moiety, s, 1H), Ar-OH at 7.8. ^{13}C NMR (DMSO- d_6 , δ , ppm): 150.2 (C₁₇), 117.5 (C₁₈), 128.3 (C₁₉), 122.6 (C₂₀), 115.5 (C₂₁), 141.9 (C₂₂), 160.3 (C₂₃), 120.2 (C₂₄), 132.4 (C₂₅), 121.8 (C₂₆), 132.1 (C₂₇), 117.8 (C₂₈), 161.6 (C₂₉).

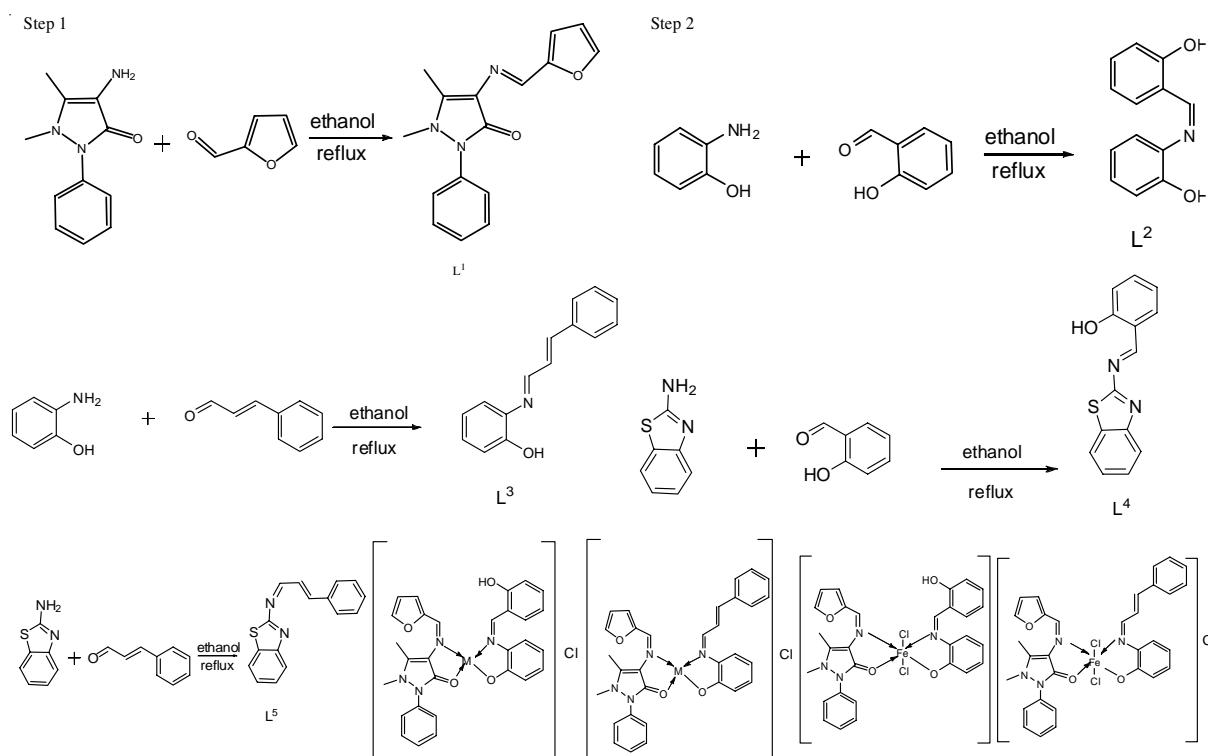
L^3 : 1H NMR (DMSO- d_6 , δ , ppm): phenyl multiplet at 7.02-8.3 δ (m, 8H), -CH=N at 8.3 δ (phenyl moiety, s, 1H), Ar-OH at 8.2 δ . ^{13}C NMR (DMSO- d_6 , δ , ppm): 152.2 (C₁₇), 119.5 (C₁₈), 124.3 (C₁₉), 122.3 (C₂₀), 115.1 (C₂₁), 135.9 (C₂₂), 163.3 (C₂₃), 119.5 (C₂₄), 133.3 (C₂₅), 135.2 (C₂₆), 128.3 (C₂₇), 128.6 (C₂₈), 127.5 (C₂₉), 128.6 (C₃₀), 128.5 (C₂₈).

L^4 : 1H NMR (DMSO- d_6 , δ , ppm): phenyl multiplet at 7.3-8.1 δ (m, 8H), -CH=N at 8.4 d (phenyl moiety, s, 1H). ^{13}C NMR (DMSO- d_6 , δ , ppm): 148.7 (C₁₇), 121.5 (C₁₈), 125.3 (C₁₉), 124.5 (C₂₀), 121.1 (C₂₁), 125.9 (C₂₂), 174.3 (C₂₃), 160.2 (C₂₄), 120.5 (C₂₅), 132.5 (C₂₆), 121.3 (C₂₇), 132.3 (C₂₈), 117.8 (C₂₉), 161.3 (C₃₀).

L^5 : 1H NMR (DMSO- d_6 , δ , ppm): phenyl multiplet at 7.3-8.1 δ (m, 8H), -CH=N at 7.5 δ (phenyl moiety, s, 1H), (6.8, 1H, phenyl C₂₄-H), (7.2, 1H, phenyl C₂₅-H). ^{13}C NMR (DMSO- d_6 , δ , ppm): 125.2 (C₁₇), 121.5 (C₁₈), 124.3 (C₁₉), 125.3 (C₂₀), 121.1 (C₂₁), 148.9 (C₂₂), 174.6 (C₂₃), 163.7 (C₂₄), 119.9 (C₂₅), 133.5 (C₂₆), 135.2 (C₂₇), 128.5 (C₂₈), 128.6 (C₂₉), 127.9 (C₃₀), 128.6 (C₃₁), 128.5 (C₃₂).

Preparation of metal complexes: An ethanolic solution of the corresponding metal chlorides ($M = FeCl_3 \cdot 6H_2O$, $CoCl_2 \cdot 6H_2O$, $NiCl_2 \cdot 6H_2O$, $CuCl_2 \cdot 2H_2O$ and $ZnCl_2$) (1 mM) was stirred with an ethanolic solution of ligand (s) (L^1 & $L^2/L^3/L^4/L^5$) (1 mM) and the resultant mixture was refluxed for about 6-8 h. Then, the volume of solution was reduced to one-third on a water bath. The solid complex precipitated was filtered, washed thoroughly with ethanol and dried *in vacuo*. The schematic route for synthesis of Schiff base ligands and their metal complexes is given in **Scheme-I**.

[ZnL¹L²]Cl (5): 1H NMR (DMSO- d_6 , δ , ppm): phenyl multiplet at 6.9-7.37 δ (m, 5H), -CH=N at 7.9 (furfuryl moiety, s, 1H), -C-CH₃ at 2.4 δ (s, 3H), N-CH₃ at 3.2 d (s, 3H), furfuryl



Scheme-I: Schematic route for synthesis of Schiff base ligands and its metal complexes

protons at 6.5-7.7 δ (m, 3H). L²: ¹H NMR (DMSO-*d*₆, δ , ppm): phenyl multiplet at 6.9-7.6 d (m, 8H), -CH=N at 8.5 δ (phenyl moiety, s, 1H).

[NiL¹ L²]Cl (3): ¹H NMR (DMSO-*d*₆, δ , ppm): phenyl multiplet at 6.9-7.37 d (m, 5H), -CH=N at 7.9 (furfuryl moiety, s, 1H), -C-CH₃ at 2.4 δ (s, 3H), N-CH₃ at 3.2 δ (s, 3H), furfuryl protons at 6.5-7.7 δ (m, 3H). L²: ¹H NMR (DMSO-*d*₆, δ , ppm): phenyl multiplet at 6.9-7.6 d (m, 8H), -CH=N at 8.4 δ (phenyl moiety, s, 1H).

DNA-binding assay: Interaction of complex with calf thymus DNA has been studied by recording electronic absorption spectra. A solution of CT-DNA in 5 mM *tris*-HCl/50 mM NaCl (pH 7) gave a ratio of UV absorbance at 260 and 280 nm (A_{260}/A_{280}) of 1.8-1.9, indicating that the DNA is free of proteins. A concentrated stock solution of DNA was prepared in 5 mM *tris*-HCl/50 mM NaCl in water at pH 7 and the concentration of CT-DNA was determined per nucleotide by taking the absorption coefficient ($6600 \text{ dm}^3 \text{ mol}^{-1} \text{ cm}^{-1}$) at 260 nm. Double distilled water was used to prepare buffer solutions. Solutions were prepared by mixing the complex and CT-DNA in DMSO medium. After equilibrium is reached (about 5 min) the spectra were recorded against an analogous blank solution containing the same concentration of DNA. UV spectral data were fitted into eqn. 1 to obtain the intrinsic binding constant (K_b)

$$[\text{DNA}]/(\epsilon_a - \epsilon_f) = [\text{DNA}]/(\epsilon_b - \epsilon_f) + K_b (\epsilon_b - \epsilon_f) \quad (1)$$

where [DNA] is the concentration of DNA in base pairs, ϵ_a , ϵ_b and ϵ_f are apparent extinction coefficient ($A_{\text{obs}}/[M]$), the extinction coefficient for the metal (M) complex in the fully bound form and the extinction coefficient for free metal (M), respectively. A plot of $[\text{DNA}]/(\epsilon_a - \epsilon_f)$ versus [DNA] gave a slope of $1/(\epsilon_b - \epsilon_f)$ and Y-intercept equal to $1/K_b (\epsilon_b - \epsilon_f)$; K_b is the ratio of the intercept.

Viscosity study: Viscosity measurements of metal complexes in the absence and the presence of DNA were carried on an Ostwald viscometer, immersed in a thermostated water-bath maintained at constant temperature at 25 ± 0.1 °C. Each experiment was performed three times and an average flow time was calculated. Data were presented as (η/η_0) versus binding ratio, where η is the viscosity of DNA in presence of complex and η_0 is the viscosity of DNA alone.

Thermal denaturation studies: Melting studies were carried out by monitoring the absorption of CT-DNA at 260 nm various temperatures in the presence and absence of each complex. The temperature of the solution was increased by 1 °C min^{-1} . The melting temperature (T_m , the temperature at which 50 % of double stranded DNA becomes single stranded) and the curve width (σ_T , the temperature range between which 10 and 90 % of the absorption increases occurred) were recorded and summarized.

Free radical scavenging activity by DPPH assay: A stock solution (1 mg/mL) was diluted to final concentrations of 20-100 $\mu\text{g}/\text{mL}$. An ethanolic DPPH solution (1 mL, 0.3 mM) was added to sample solutions in DMSO (3 mL) at various concentrations (50-300 $\mu\text{g}/\text{mL}$)³⁴. The mixture was shaken vigorously and allowed to stand at room temperature for 30 min. The absorbance was then measured at 517 nm using the UV-visible, spectrophotometer. Less absorbance by the reaction mixture indicates higher free-radical-scavenging activity. DMSO was used as the solvent and ascorbic acid as the standard. The DPPH radical scavenger effect was calculated using the following eqn:

$$\text{Scavenging effect (\%)} = ((A_0 - A_1)/A_0) \times 100 \quad (2)$$

where A_0 is the absorbance of the control reaction and A_1 is the absorbance in the presence of the samples or standard.

Superoxide dismutase activity: *in vitro* Superoxide dismutase activity was measured using alkaline DMSO as a source of superoxide radical ion ($O_2^{\cdot-}$) and nitrobluetetrazolium (NBT) as $O_2^{\cdot-}$ scavenger³⁵. In general, 400 μ L of the sample to be assayed was added to a solution containing 2.1 mL of 0.2 M potassium phosphate buffer (pH 7.8) and 1 mL of 56 μ M NBT. The tubes were kept in ice for 20 min and then 1.5 mL of alkaline DMSO solution was added while stirring. The absorbance was then monitored at 560 nm against a sample prepared under similar condition except that NaOH was absent in DMSO. The percent inhibition was calculated from the following eqn:

$$\% \text{ Inhibition} = ((C-T) \times 100)/C \quad (3)$$

where C and T are the optical density of the control and test samples, respectively.

Reducing power: The complexes (25-800 mM) in DMSO were mixed with 2.5 mL of phosphate buffer (0.2 M, pH 6.6) and 2.5 mL potassium ferricyanide [$K_3Fe(CN)_6$] (1 %) and then the mixture was incubated at 50 °C for 0.5 h afterwards, 2.5 mL of trichloroacetic acid (10 %) was added to the mixture, which was then centrifuged at 3000 rpm for 10 min. Finally, 2.5 mL distilled water and 0.5 mL $FeCl_3$ (0.1 %) and the absorbance was measured at 700 nm. Increased absorbance of the reaction mixture indicated increased reducing power.

Antimicrobial activity: The *in vitro* evaluation of antimicrobial activity was carried out. The synthesized compounds were tested against some fungi and bacteria to provide minimum inhibitory concentration for each compound. Minimum inhibitory concentration is the lowest concentration of solution to inhibit the growth of a test organism. The *in vitro* biological

screening effects of the investigated compounds were tested against the bacterial species *Staphylococcus aureus*, *Escherichia coli*, *Klebsiella pneumoniae*, *Salmonella typhi* and *Pseudomonas aeruginosa* and fungal species *Aspergillus niger*, *Rhizopus stolonifer*, *Aspergillus flavus*, *Rhizoctonia bataicola* and *Candida albicans* by disc diffusion method. Pencillin ampicillin, vancomycin, ofloxacin were used as standards for antibacterial activity. Nystatin, ketoconazole, clotrimazole was used as standard for antifungal activity, respectively. The test organisms were grown on nutrient agar medium in petri plates. The compounds were prepared in DMSO and soaked in a filter paper disc of 5 mm diameter and 1 mm thickness. The compounds were prepared in DMSO and soaked in a filter paper disc of 5 mm diameter and 1 mm thickness. The discs were placed on the previously seeded plates and incubated at 37 °C and the diameter of inhibition zone around each disc was measured after 24 h for antibacterial and 72 h for antifungal activities. The minimum inhibitory concentration was determined by serial dilution technique.

RESULTS AND DISCUSSION

The analytical data and physical properties of the Schiff base ligands (L^1 - L^5) and its metal complexes are listed in Table-1. The resulting metal complexes were found to be stable at room temperature and soluble in common organic solvents. The elemental analysis data (Table-1) confirmed that the complexes have a 1:1:1 molar ratio between the metal and the Schiff base ligands. The molar conductance of all the complexes was measured in DMSO using 10^{-3} M solutions at room temperature. The conductance (Table-1) values are found to be in the range

TABLE-1
PHYSICAL AND ANALYTICAL DATA OF THE SYNTHESIZED METAL COMPLEXES

Compound/m.f.	Colour	Yield (%)	Elemental analysis (%): Found (calcd.)					Molar conductance ($\Omega^{-1} \text{ cm}^2 \text{ mol}^{-1}$)	μ_{eff} (B.M.)
			C	H	N	Cl	M		
L^1	Yellow	85	68.30 (68.31)	5.35 (5.37)	14.91 (14.94)	-	-	-	-
L^2	Yellow	82	73.20 (73.21)	5.21 (5.20)	6.59 (6.57)	-	-	-	-
L^3	Dark Yellow	81	80.65 (80.68)	5.89 (5.87)	6.25 (6.28)	-	-	-	-
L^4	Dark Yellow	84	66.12 (66.13)	3.98 (3.97)	11.01 (11.02)	-	-	-	-
L^5	Yellow	81	72.70 (72.71)	4.47 (4.58)	10.64 (10.61)	-	-	-	-
[$FeL^1L^2Cl_2$] (1) $C_{29}H_{25}Cl_2FeN_4O_4$	Brown	83	56.15 (56.13)	4.02 (4.06)	9.03 (9.04)	11.45 (11.44)	8.98 (9.01)	7	5.81
[CoL^1L^2Cl] (2) $C_{29}H_{25}ClCoN_4O_4$	Dark Brown	82	59.21 (59.23)	4.25 (4.29)	9.56 (9.53)	6.04 (6.03)	10.05 (10.03)	38	3.85
[NiL^1L^2Cl] (3) $C_{29}H_{25}ClNiN_4O_4$	Dark Green	84	59.23 (59.25)	4.25 (4.29)	9.50 (9.54)	6.01 (6.04)	9.97 (9.99)	45	Dia
[CuL^1L^2Cl] (4) $C_{29}H_{25}ClCuN_4O_4$	Green	86	58.75 (58.77)	4.21 (4.25)	9.45 (9.46)	5.97 (5.99)	10.74 (10.73)	35	1.83
[ZnL^1L^2Cl] (5) $C_{29}H_{25}ClZnN_4O_4$	Dark Brown	84	58.56 (58.58)	4.23 (4.24)	9.40 (9.43)	5.99 (5.97)	10.97 (11.01)	46	Dia
[$FeL^1L^3Cl_2$] (6) $C_{31}H_{27}Cl_2FeN_4O_3$	Brown	83	59.01 (59.05)	4.35 (4.32)	8.87 (8.89)	11.21 (11.26)	8.89 (8.87)	5	5.87
[CoL^1L^3Cl] (7) $C_{31}H_{27}ClCoN_4O_3$	Dark Brown	82	62.23 (62.25)	4.54 (4.55)	9.34 (9.37)	5.94 (5.93)	9.87 (9.86)	32	3.81
[NiL^1L^3Cl] (8) $C_{31}H_{27}ClNiN_4O_3$	Green	81	62.25 (62.27)	4.51 (4.56)	9.38 (9.38)	5.95 (5.94)	9.84 (9.83)	43	Dia
[CuL^1L^3Cl] (9) $C_{31}H_{27}ClCuN_4O_3$	Dark Green	84	61.78 (61.77)	4.55 (4.52)	9.27 (9.30)	5.87 (5.89)	10.54 (10.55)	31	1.79

Compound/m.f.	Colour	Yield (%)	Elemental analysis found (Calcd.) (%)					Molar conductance ($\Omega^{-1}\text{cm}^2 \text{mol}^{-1}$)	μ_{eff} (B.M.)
			C	H	N	Cl	M		
[ZnL ¹ L ³]Cl (10) C ₃₁ H ₂₇ ClZnN ₄ O ₃	Brown	87	61.59 (61.58)	4.54 (4.50)	9.28 (9.27)	5.84 (5.87)	10.82 (10.83)	49	Dia
[FeL ¹ L ⁴ Cl ₃] (11) C ₃₀ H ₂₅ Cl ₃ FeN ₅ O ₃ S	Brown	78	51.64 (51.62)	3.63 (3.61)	10.09 (10.04)	15.23 (15.25)	8.05 (8.01)	9	5.76
[CoL ¹ L ⁴ Cl]Cl (12) C ₃₀ H ₂₅ Cl ₂ CoN ₅ O ₃ S	Brown	81	(54.15)(54.13)	3.73 (3.79)	10.54 (10.53)	10.65 (10.66)	8.88 (8.86)	34	3.91
[NiL ¹ L ⁴ Cl]Cl (13) C ₃₀ H ₂₅ Cl ₂ NiN ₅ O ₃ S	Dark Yellow	85	54.4 (54.15)	3.74 (3.79)	10.55 (10.53)	10.65 (10.67)	8.82 (8.83)	41	Dia
[CuL ¹ L ⁴ Cl]Cl (14) C ₃₀ H ₂₅ Cl ₂ CuN ₅ O ₃ S	Dark Green	83	53.78 (53.76)	3.75 (3.76)	10.44 (10.46)	10.58 (10.59)	9.46 (9.49)	38	1.80
[ZnL ¹ L ⁴ Cl]Cl(15) C ₃₀ H ₂₅ Cl ₂ ZnN ₅ O ₃ S	Green	82	53.64 (53.61)	3.78 (3.75)	10.44 (10.43)	10.58 (10.56)	9.79 (9.74)	47	Dia
[FeL ¹ L ⁵ Cl ₃] (16) C ₃₂ H ₂₇ Cl ₃ FeN ₅ O ₂ S	Dark Brown	73	54.24 (54.28)	3.86 (3.85)	9.93 (9.90)	15.06 (15.04)	7.85 (7.89)	4	5.85
[CoL ¹ L ⁵ Cl]Cl (17) C ₃₂ H ₂₇ Cl ₂ CoN ₅ O ₂ S	Dark Yellow	80	56.85 (56.89)	4.04 (4.03)	10.36 (10.37)	10.53 (10.50)	8.74 (8.73)	37	3.73
[NiL ¹ L ⁵ Cl]Cl (18) C ₃₂ H ₂₇ Cl ₂ NiN ₅ O ₂ S	Dark Brown	79	56.94 (56.91)	4.08 (4.03)	10.36 (10.38)	10.56 (10.51)	8.76 (8.70)	49	Dia
[CuL ¹ L ⁵ Cl]Cl (19) C ₃₂ H ₂₇ Cl ₂ CuN ₅ O ₂ S	Green	81	56.53 (56.50)	4.24 (4.20)	10.35 (10.30)	10.41 (10.43)	9.38 (9.35)	34	1.82
[ZnL ¹ L ⁵ Cl]Cl (20) C ₃₂ H ₂₇ Cl ₂ ZnN ₅ O ₂ S	Yellow	83	56.33 (56.35)	3.94 (3.99)	10.24 (10.27)	10.43 (10.40)	9.63 (9.60)	51	Dia

of 4-51 ($\Omega^{-1} \text{cm}^2 \text{mol}^{-1}$), indicating that all the complexes are 1:1 electrolytic in nature except iron complex (non electrolytic in nature)³⁶. In addition, the presence of coordinated chloride is confirmed by the silver nitrate test. The purity of ligands and their metal complexes has been checked by TLC.

IR spectra: Determination of the coordinating atoms was done on the basis of the comparison of IR spectra of ligands and of the mixed ligand complexes. Significant wave numbers are given in Table-2.

The strong band at 1717 cm^{-1} of the $\nu(\text{C}=\text{O})$ in L¹ free ligand, which is shifted to 1699-1684 cm^{-1} in complexes suggesting that the carbonyl oxygen is coordinated.

The bands at 1616 and 1635 cm^{-1} in the L¹ and L² ligands, respectively are attributed to $\nu(\text{HC}=\text{N})$ stretching vibrations. On coordination, these bands are shifted towards lower values in (1599-1586 and 1593-1586 cm^{-1}) which suggest that the ligand(s) are coordinated to metal ion *via* azomethane nitrogen in all complexes. This change in shift is due to the drift of the

TABLE-2
IR SPECTRAL DATA (cm^{-1}) FOR THE FREE LIGANDS AND THEIR METAL COMPLEXES

Compound/ m.f	$\nu_{\text{C}=\text{O}}$ (cm^{-1})	$\nu_{\text{C}=\text{N}}$ (cm^{-1})	$\nu_{\text{M}=\text{O}}$ (cm^{-1})	$\nu_{\text{M}=\text{N}}$ (cm^{-1})	$\nu_{\text{M}=\text{Cl}}$ (cm^{-1})	Compound/ m.f	$\nu_{\text{C}=\text{O}}$ (cm^{-1})	$\nu_{\text{C}=\text{N}}$ (cm^{-1})	$\nu_{\text{M}=\text{O}}$ (cm^{-1})	$\nu_{\text{M}=\text{N}}$ (cm^{-1})	$\nu_{\text{M}=\text{Cl}}$ (cm^{-1})
L ¹	1717	1616	-	-	-	[CuL ¹ L ³]Cl(9) C ₃₁ H ₂₇ ClCuN ₄ O ₃	1689	1593	531	469	-
L ²	-	1635	-	-	-	[ZnL ¹ L ³]Cl(10) C ₃₁ H ₂₇ ClZnN ₄ O ₃	1698	1595	542	467	-
L ³	-	1628	-	-	-	[FeL ¹ L ⁴ Cl ₃](11) C ₃₀ H ₂₅ Cl ₃ FeN ₅ O ₃ S	1686	1595	526	477	359
L ⁴	-	1642	-	-	-	[CoL ¹ L ⁴ Cl]Cl(12) C ₃₀ H ₂₅ Cl ₂ CoN ₅ O ₃ S	1695	1596	529	480	-
L ⁵	-	1638	-	-	-	[NiL ¹ L ⁴ Cl]Cl(13) C ₃₀ H ₂₅ Cl ₂ NiN ₅ O ₃ S	1698	1594	535	475	-
[FeL ¹ L ² Cl ₂](1) C ₂₉ H ₂₅ Cl ₂ FeN ₄ O ₄	1693	1596	530	476	343	[CuL ¹ L ⁴ Cl]Cl(14) C ₃₀ H ₂₅ Cl ₂ CuN ₅ O ₃ S	1696	1595	545	481	-
[CoL ¹ L ²]Cl (2) C ₂₉ H ₂₅ ClCoN ₄ O ₄	1691	1594	528	471	-	[ZnL ¹ L ⁴ Cl]Cl(15) C ₃₀ H ₂₅ Cl ₂ ZnN ₅ O ₃ S	1684	1591	543	464	-
[NiL ¹ L ²]Cl(3) C ₂₉ H ₂₅ ClNiN ₄ O ₄	1694	1597	546	465	-	[FeL ¹ L ⁵ Cl ₃](16) C ₃₂ H ₂₇ Cl ₃ FeN ₅ O ₂ S	1685	1596	537	473	371
[CuL ¹ L ²]Cl(4) C ₂₉ H ₂₅ ClCuN ₄ O ₄	1690	1591	532	463	-	[CoL ¹ L ⁵ Cl]Cl(17) C ₃₂ H ₂₇ Cl ₂ CoN ₅ O ₂ S	1699	1586	541	468	-
[ZnL ¹ L ²]Cl(5) C ₂₉ H ₂₅ ClZnN ₄ O ₄	1692	1593	527	470	-	[NiL ¹ L ² Cl]Cl(18) C ₃₂ H ₂₇ Cl ₂ NiN ₅ O ₂ S	1686	1592	536	474	-
[FeL ¹ L ³ Cl ₂](6) C ₃₁ H ₂₇ Cl ₂ FeN ₄ O ₃	1695	1595	534	466	347	[CuL ¹ L ⁵ Cl]Cl(19) C ₃₂ H ₂₇ Cl ₂ CuN ₅ O ₂ S	1687	1590	544	479	-
[CoL ¹ L ³]Cl (7) C ₃₁ H ₂₇ ClCoN ₄ O ₃	1697	1596	540	478	-	[ZnL ¹ L ⁵ Cl]Cl(20) C ₃₂ H ₂₇ Cl ₂ ZnN ₅ O ₂ S	1695	1588	539	471	-
[NiL ¹ L ³]Cl(8) C ₃₁ H ₂₇ ClNiN ₄ O ₃	1688	1599	538	472	-	—	—	—	—	—	—

TABLE-3
ELECTRONIC ABSORPTION SPECTRAL DATA OF THE COMPLEXES IN DMSO SOLUTION

Comp.	Solvent	Absorption (nm)	Band assignment	Geometry	Comp.	Solvent	Absorption (nm)	Band assignment	Geometry
L ¹	DMSO	265	$\pi-\pi^*$	-	[FeL ¹ L ² Cl ₂] (1)	DMSO	325 749	$n-\pi^*$ ${}^6A_{1g} \rightarrow {}^4T_{1g}$	Octahedral
L ²	DMSO	335	$N-\pi^*$	-	[CoL ¹ L ²]Cl (2)	DMSO	348 560	$n-\pi^*$ ${}^1A_{1g} \rightarrow {}^1B_g$	Square planar
L ³	DMSO	243	$\pi-\pi^*$	-	[NiL ¹ L ²]Cl (3)	DMSO	238 430	$\pi-\pi^*$ ${}^1A_{1g} \rightarrow {}^1B_{1g}$	Square planar
L ⁴	DMSO	319	$\pi-\pi^*$	-	[CuL ¹ L ²]Cl (4)	DMSO	352 445	$n-\pi^*$ ${}^2B_{1g} \rightarrow {}^2A_{1g}$	Square planar
L ⁵	DMSO	357	$n-\pi^*$	-	[ZnL ¹ L ²]Cl (5)	DMSO	523	$L \rightarrow M$	Square planar

lone pair density of azomethane nitrogen towards metal atom. The OH stretching vibration of the ligand (L²) was appeared at the range (3441-3228 cm⁻¹), while it disappeared in the IR-spectra of the Schiff-base complexes due to the coordination of the metal ion to the oxygen of the ligand. The coordination through nitrogen of azomethine and oxygen of $\nu(C-O)$ of ligand are further evidenced by the appearance in the complexes of non-ligand bands around 546-527 and 463-476 cm⁻¹ are due to $\nu(M-O)$ and $\nu(M-N)$ bond. Furthermore, the IR spectra of the Fe(III) show another band in the region 343 cm⁻¹, which is due to $\nu(Fe-Cl)$ vibrations.

Electronic absorption spectra: The electronic absorption spectral data of the ligands and their complexes (1-5) were recorded in DMSO and presented in Table-3. The electronic absorption spectra are very helpful in the evaluation of results furnished by other methods of structural investigation. The electronic spectral measurements were used for assigning the stereochemistries of metal ions in the complexes based on the positions and number of *d-d* transition peaks. There are two absorption bands, assigned to $n-\pi^*$ and $\pi-\pi^*$ transitions, in the electronic spectrum of the ligands. These transitions are also found in the spectra of the complexes, but they are shifted towards lower and higher frequencies, confirming the coordination of the ligand to the metallic ions.

Fe(III) complex exhibit bands at 325 and 749 nm assignable to $n-\pi^*$ and ${}^6A_{1g} \rightarrow {}^4T_{1g}(G)$, respectively. The observed magnetic moment 5.81 BM along with electronic transitions corresponds to octahedral geometry.

The cobalt complex shows a *d-d* band at 348 and 560 nm assigned to $n-\pi^*$ and ${}^1A_{1g} \rightarrow {}^1B_{1g}$ transition, which confirms square-planar geometry. This is further confirmed by its magnetic susceptibility value (3.85 BM).

The nickel complex is diamagnetic suggesting square-planar geometry. The electronic absorption spectrum of the nickel complex shows a *d-d* band at 238 and 430 nm assigned as $n-\pi^*$ and ${}^1A_{1g} \rightarrow {}^1B_{1g}$ transition³⁷, which also indicates the square planar geometry.

The electronic spectra of copper complex in DMSO solution displays a broad band at 352 nm and a well-defined shoulder around 445 nm, attributable to $n-\pi^*$ and ${}^2B_{1g} \rightarrow {}^2A_{1g}$ transitions which strongly favour square-planar geometry around the central metal ion. This is further supported by the magnetic susceptibility value (1.83 BM)³⁸⁻⁴⁰.

Zn(II) is a *d*¹⁰ metal ion, no band is expected in the visible region and is also found as a diamagnetic complex, as expected.

However, a strong band observed at 523 nm is assignable to the $L \rightarrow M$ charge transfer transition⁴¹ which is compatible with this complex having a square planar geometry.

ESR spectra: The EPR spectra of metal chelates provide information about hyperfine and super hyperfine structures which are of importance in studying the metal ion environment in the complexes *i.e.*, the geometry, nature of the coordinating sites of the Schiff base and the metal and the degree of covalency of the metal ligand bonds. ESR spectrum of the Cu(II) complex (4) was recorded in DMSO at 300 and 77 K (Fig. 1). The spectrum of the above Cu(II) complex at 300 K shows one intense absorption band in the high field region, which is isotropic due to the tumbling motion of the molecules. However, this complex in the frozen solution shows four well resolved peaks with low intensities in the low field region. No band corresponding to the $\Delta m_s = \pm 2$ transition was observed in the spectra, ruling out any Cu-Cu interaction. The observed trend of $g_{||}(2.23) > g_{\perp}(2.02) > g_e(2.0023)$ describes the axial symmetry with the unpaired electron residing in the $d_{x^2-y^2}$ orbital⁴².

In axial spectra, the *g*-values are related with exchange coupling constant (*G*) by the expression

$$G = g_{||} - 2.0023/g_{\perp} - 2.0023 \quad (4)$$

According to Hathaway and Billing⁴², if the *G* is larger than four, exchange interaction is negligible because the local tetragonal axis is mixligand. For the present copper complex, the *G* value is 4.8, which suggests that the local tetragonal axis is aligned parallel or slightly misaligned and consistent with $d_{x^2-y^2}$ ground state. EPR and optical spectra have been used to determine the covalent bonding parameters for the Cu(II) ion in various environments. Since there has been wide interest in the nature of bonding parameters in the system, we adopted the simplified molecular orbital theory⁴³ to calculate the bonding coefficients such as in-plane π bonding (β^2) and in-plane σ -bonding (α^2). The in-plane σ -bonding parameter, α^2 is related to $g_{||}$ and g_{\perp} according to the following equation: $\alpha^2 = (A_{||}/0.036) + (g_{||} - 2.0027) + 3/7 (g_{\perp} - 2.0023) + 0.04$ (5)

If the α^2 value is 0.5, it indicates a complete covalent bonding, while the value of $\alpha^2 = 1.0$ suggests a complete ionic bonding. The observed value of α^2 (0.76) indicates that the complex has some covalent character. The in-plane π -bonding (β^2) and out-plane π -bonding (γ^2) parameters are calculated from the following equations:

$$\beta^2 = (g_{||} - 2.0027) E / -8\lambda \alpha^2 \quad (6)$$

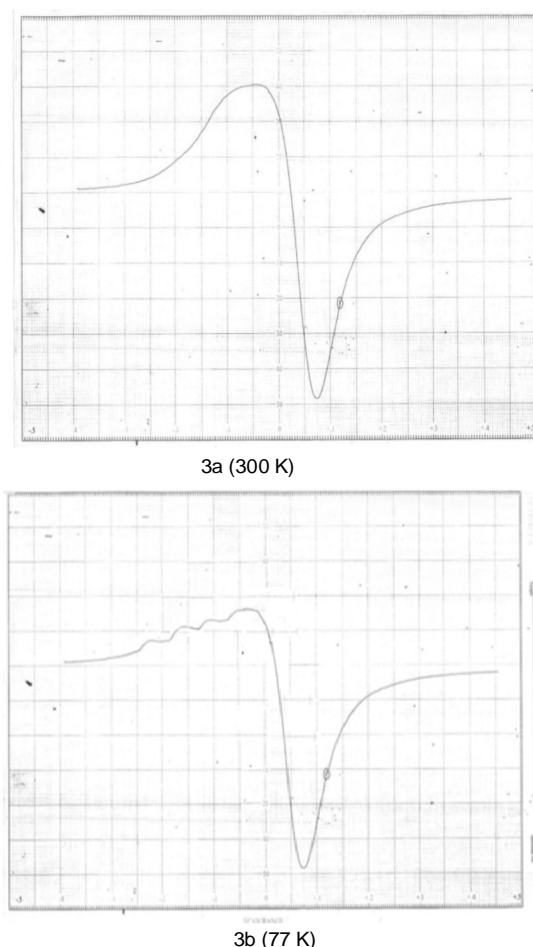


Fig. 1. ESR spectra of copper complex at 300 K; (a) 77 K (3b)

$$\gamma^2 = (g_{\parallel} - 2.0027) E / -2\lambda \alpha^2 \quad (7)$$

where $\lambda = -828 \text{ cm}^{-1}$ for the free metal ion. The observed β^2 (1.2) and γ^2 (0.83) values indicate that there is interaction in the out-plane π -bonding, whereas in-plane π -bonding is completely ionic. This is also confirmed by orbital reduction factors (K_{\parallel} and K_{\perp}) which are calculated from the following equations:

$$K_{\parallel} = \alpha^2 \beta^2 \quad (8)$$

$$K_{\perp} = a^2 \gamma^2 \quad (9)$$

For the present complex, the observed order K_{\parallel} (0.91) $>$ K_{\perp} (0.63) implies a greater contribution from out-of plane π -bonding than from in-plane π -bonding in metal-ligand π -bonding. The A_{\parallel} and A_{\perp} values in the order: A_{\parallel} (148) $>$ A_{\perp} (47) also indicate that the complex has square planar geometry. The empirical factor $f = g_{\parallel}/A_{\parallel} \text{ cm}^{-1}$ is an index of tetragonal distortion. Values of this factor may vary from 105 to 135 for

small to extreme distortions in square planar complexes and it depends on the nature of the coordinated atoms⁴⁴. The f values of copper complexes^{4,9,14} found to be in the range 150, 145, 146 and 149 (Table-4) indicating significant distortion from planarity.

DSC analysis: DSC curves presented a melting process for Cu(II) complex and the decomposition is represented by exothermic processes shown in Fig. 2. The thermal stability observed in the order; Zn(II) complex $>$ Cu(II) complex $>$ Co(II) complex $>$ Ni(II) complex $>$ Fe(III) complex $>$ Zn(II) complex.

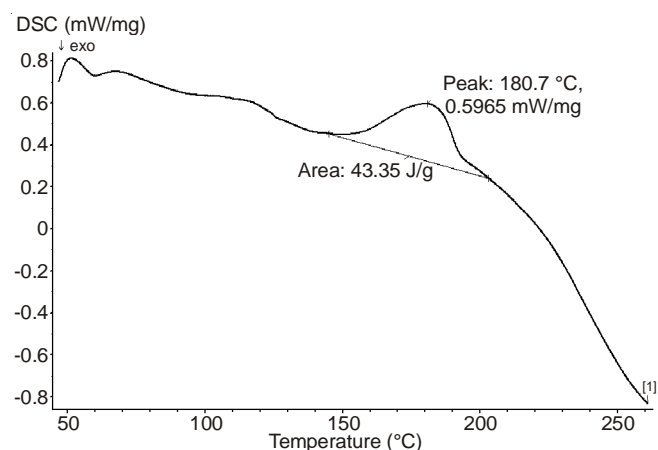


Fig. 2. DSC curve of Cu(II) complex

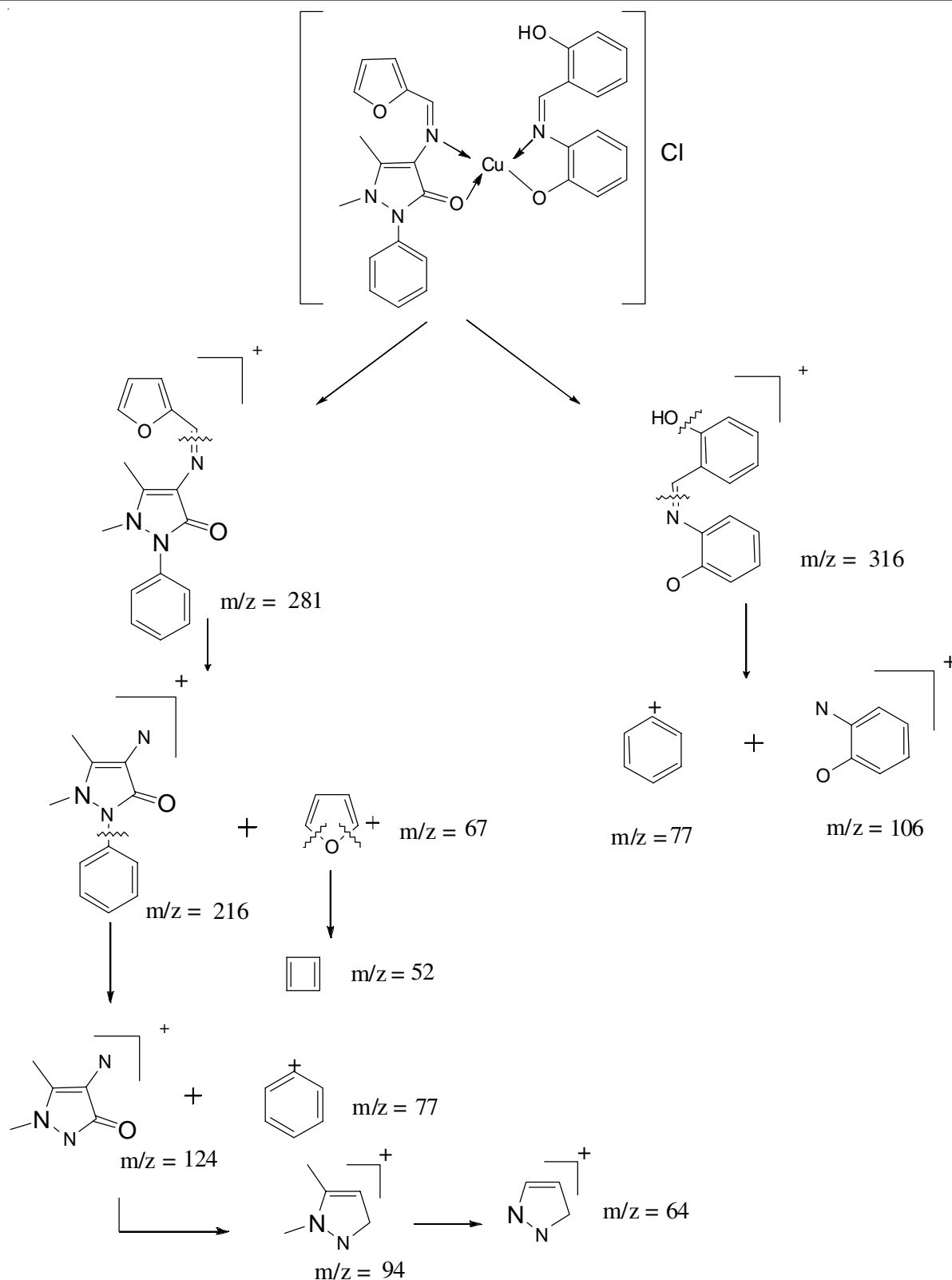
Mass spectra: The FAB mass spectra of the Schiff bases and their corresponding metal complexes were recorded and compared their stoichiometry compositions (**Scheme-II**). In the present investigations, the mass spectrum of the Schiff base ligands L^1 and L^2 shows the formation of molecular ion peak at $m/z = 281$ & 213 corresponding to the total molecular weight of the ligand. The mass spectra of Fe(III), Co(II), Ni(II), Cu(II) and Zn(II) complexes show a molecular ion peak (M^+) at m/z 620, 588, 587, 592 and 594, respectively, the stoichiometry of the complexes as supported by the FAB mass spectra of other complexes. Elemental analysis values are in close agreement with the values calculated from molecular formula of these complexes, which is further supported by the FAB-mass studies of representative complexes.

DNA binding studies: The ability of complexes to bind the DNA was investigated by electronic absorption spectra, viscosity, thermal denaturation and cyclic voltammetry techniques.

Absorption spectral features of DNA binding: The DNA binding studies of the mixed ligand complexes were studied using absorption spectra. In general, hypochromism

TABLE-4
ESR SPECTRAL DATA OF THE COPPER COMPLEX

Complex	G_{\parallel}	G_{\perp}	g_{iso}	A_{\parallel}	A_{\perp}	K_{\parallel}	K_{\perp}	α^2	β^2	γ^2	$f = (g_{\parallel}/A_{\parallel})$
[CuL ¹ L ²]Cl (4) at 300 K	—	—	2.04	—	—	—	—	—	—	—	—
[CuL ¹ L ²]Cl at 77 K	2.23	2.02	—	148	47	0.91	0.63	0.76	1.2	0.83	150
[CuL ¹ L ³]Cl (9) at 300 K	—	—	2.09	—	—	—	—	—	—	—	—
[CuL ¹ L ³]Cl at 77 K	2.24	2.05	—	155	42	1.1	0.63	0.78	1.4	0.82	145
[CuL ¹ L ⁴]Cl (14) at 300 K	—	—	2.08	—	—	—	—	—	—	—	—
[CuL ¹ L ⁴]Cl at 77 K	2.28	2.07	—	156	45	0.83	0.63	0.75	1.1	0.84	146
[CuL ¹ L ⁵]Cl at 77 K	—	—	2.03	—	—	—	—	—	—	—	—
[CuL ¹ L ⁵]Cl at 300 K	2.25	2.04	—	151	43	0.94	0.62	0.73	1.3	0.86	149



and red-shift are associated with the binding of the complex to the helix by an intercalative mode involving strong stacking interaction of the aromatic chromophore of the complex between the DNA base pairs. The absorption intensity of the mixed ligand complex was decreased (hypochromism) after the addition of DNA, which indicated the interactions between DNA and the complex. We have observed minor red shift along

with significant hypochromicity for the complex. The spectroscopic changes suggested that the complex has interaction with DNA. After the complex intercalate with the base pairs of DNA, the π^* orbital could couple with p orbitals of the base pairs, which decreasing the $\pi \rightarrow \pi^*$ transition energies. The result shows that the absorbance (hypochromism) decreased by the successive addition of CT- DNA to the complex solution.

The hypochromism and bathochromic shift are observed for the complexes suggesting that binding is intercalative mode. The absorption spectra of complexes in the absence and presence of CT-DNA of complexes (**1-5**) are investigated. The observed K_b values for metal complexes (**1-15**) are equal to the classical intercalators bound to CT-DNA. The K_b values for complex ($1.2 \times 10^6 \text{ M}^{-1}$, $1 \times 10^6 \text{ M}^{-1}$, $1.3 \times 10^6 \text{ M}^{-1}$, $1.5 \times 10^6 \text{ M}^{-1}$ and $1.1 \times 10^6 \text{ M}^{-1}$, respectively). The binding constants of these metal complexes were compared to typical classical intercalators (ethidium-DNA, $1.4 \times 10^6 \text{ M}^{-1}$)⁴⁵. The results show that the present complexes are involved in intercalative interactions with CT-DNA.

Viscosity measurements: A classical intercalation model demands that the DNA helix lengthen as base pairs are separated to accommodate the binding ligand, leading to an increase in DNA viscosity. In contrast, a partial, non-classical intercalation of compound could bend (or kink) the helix, reducing its effective length and concomitantly, its viscosity^{46,47}.

The values of relative viscosity (η/η_0) (where η and η_0 are the specific viscosities of DNA in the presence and absence of the complexes) are plotted against [complex]/[DNA] gives a measure of the viscosity changes. The effects of all the mixed ligand complexes (**1-5**) on the viscosity of CT DNA are shown in Fig. 3. The viscosity of DNA is increased with the increment of each complexes and it is similar to the behavior of well-known DNA-intercalator of the ethidium bromide. This result suggested that the mixed ligand complexes are intercalates between the base pair of DNA and also equal to the spectroscopic results such as hypochromism and bathochromism of complexes in the presence of DNA.

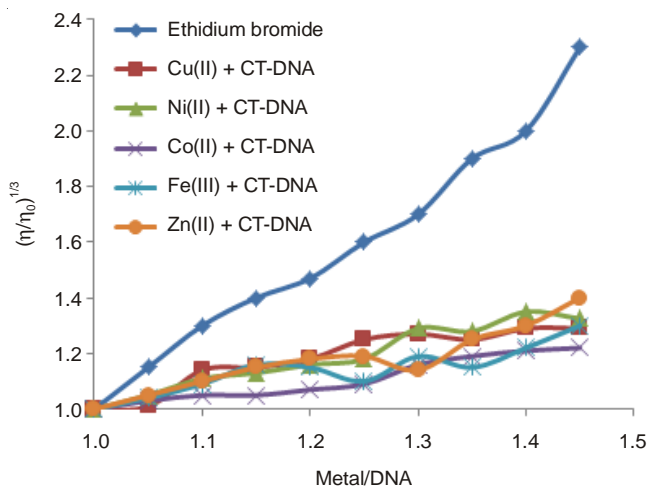


Fig. 3. Effect on relative viscosity of CT-DNA under the influence of increasing amount mixed ligand complexes at $25 \pm 0.1 \text{ }^\circ\text{C}$

Thermal denaturation studies: Thermal behaviour of DNA in the presence of mixed ligand complexes can give an insight into their conformational changes when temperature is raised and offer information about the interaction strength of complexes with DNA. It is well known that when the temperature in the solution increases, the double stranded DNA gradually dissociates to single strands and generates a hypochromic effect on the absorption spectra of DNA bases ($\lambda_{\text{max}} = 260 \text{ nm}$)⁴⁸. The melting temperature (T_m) is defined as

the temperature at which half of the DNA strands are in the double-helical state and half are in the "random-coil" state⁴⁹. According to the literature the interaction of metallointercalators generally results in a considerable increase in melting temperature (T_m). The thermal denaturation of DNA in the absence and presence of the complexes (**1-5**) is shown in Fig. 4. The T_m of calf thymus-DNA is found to be $69.5 \pm 0.1 \text{ }^\circ\text{C}$. However, with addition of complexes (**1-5**) T_m increased to 73.4 ± 1 , 73.5 ± 1 , 73.4 ± 1 , 73.6 ± 1 and $74.3 \pm 1 \text{ }^\circ\text{C}$, respectively which indicate that these compounds stabilize the double helix of DNA. The increased T_m ($3.9\text{-}4.8 \text{ }^\circ\text{C}$) value of the DNA after addition of the complexes is comparable to that observed for classical intercalators⁵⁰. This method is easy to identify when more than one transition occurs⁵¹. This transition of double stranded DNA to single stranded DNA is termed as the melting temperature of DNA (T_m)⁵². These variations in T_m of calf thymus-DNA strongly supported the intercalation of metal complex into the double helix DNA.

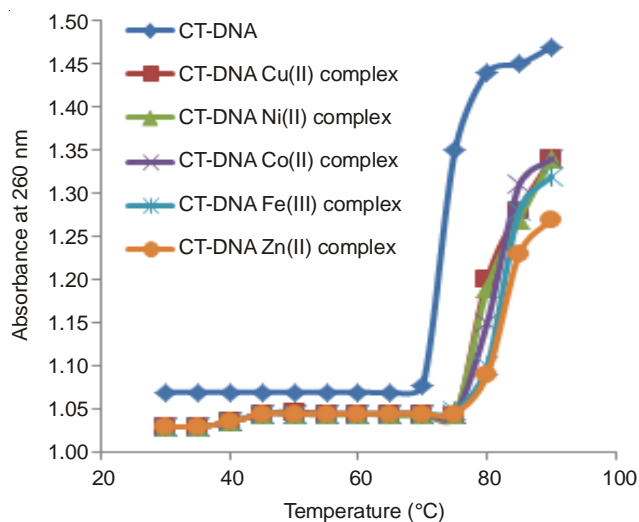


Fig. 4. Melting curves of CT-DNA in the absence and presence of complexes

DNA binding study: Cyclic voltammetry is useful technique for investigating the interaction of the metal complexes with DNA. In the cyclic voltammetric (CV) study, copper complexes in the presence and absence of CT DNA are shown in Fig. 5. In the absence of CT DNA, the first redox $E_{\text{pc}} = 0.110 \text{ V}$ for $\text{Cu(II)} \rightarrow \text{Cu(I)}$ [$E_{\text{pa}} = 0.510 \text{ V}$, $\Delta E_{\text{p}} = -0.40 \text{ V}$ and $E_{1/2} = 0.310 \text{ V}$]. The second peak, $E_{\text{pc}} = -1.10 \text{ V}$ for $\text{Cu(I)} \rightarrow \text{Cu(0)}$ [$E_{\text{pa}} = -0.745 \text{ V}$, $\Delta E_{\text{p}} = 0.355 \text{ V}$ and $E_{1/2} = -0.923 \text{ V}$]. The $i_{\text{pa}}/i_{\text{pc}}$ ratios of these redox peaks 1.12 are 1.17, respectively, which indicate that the reaction of the Cu(II) complex exhibited quasi-reversible redox process. The presence of DNA in the solution at the same concentration of Cu(II) complex causes negative shift in $E_{1/2}$ and a decrease in ΔE_{p} , which indicate that the Cu(II) complex had interacted with DNA. The value of $i_{\text{pc}}/i_{\text{pa}}$ also decreases with the increase of DNA concentration. The decrease in peak currents can be explained in terms of an equilibrium mixture of free and DNA-bound Cu(II) complex to the electrode surface. For $\text{Fe(III)} \rightarrow \text{Fe(II)}$ the peak $E_{\text{pc}} = -0.873 \text{ V}$ in the absence of CT DNA ($E_{\text{pa}} = -0.645 \text{ V}$, $\Delta E_{\text{p}} = 0.228$, $E_{1/2} = -0.759 \text{ V}$). The ratio of $i_{\text{pa}}/i_{\text{pc}}$ was approximately 1.21, indicating the quasi-reversible redox process of the metal

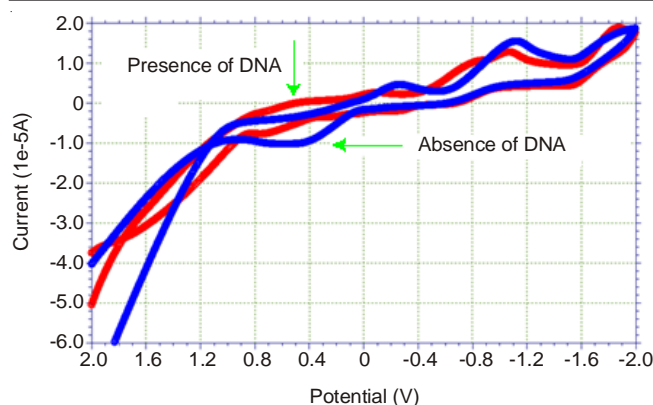


Fig. 5. Cyclic voltammogram of copper complexes in the absence and presence of DNA at various concentration. Arrow indicates the changes in voltammetric currents upon increasing the DNA concentration

complex. The incremental addition of CT DNA to the complexes the redox couples caused a negative shift in $E_{1/2}$ and a decrease in ΔE_p . For Co(II) \rightarrow Co(I) the peak $E_{pc} = -0.759$ V in the absence of CT-DNA ($E_{pa} = -0.720$ V, $\Delta E_p = 0.194$, $E_{1/2} = -0.817$ V). The ratio of i_{pa}/i_{pc} was approximately 1.28, indicating the quasi-reversible redox process of the metal complex. The incremental addition of CT-DNA to the complexes the redox couples caused a negative shift in $E_{1/2}$ and a decrease in ΔE_p . Ni(II) complex exhibited quasi-reversible transfer process with redox couple [Ni(II) \rightarrow Ni(I)], $E_{pc} = -0.782$ V in the absence of CT-DNA ($E_{pa} = -0.563$ V, $\Delta E_p = 0.219$, $E_{1/2} = -0.672$ V). The ratio of i_{pa}/i_{pc} was 1.41 V, indicating the quasi-reversible redox process of the metal complex. Incremental addition of DNA on Ni(II) complex showed a slight decrease in the current intensity and negative shift of the oxidation peak potential. Finally Zn(II) complex exhibited quasi-reversible transfer process with redox couple, [Zn(II) \rightarrow Zn(0)] cathodic peak $E_{pc} = -0.858$ V in the absence of CT-DNA ($E_{pa} = -0.572$ V, $\Delta E_p = 0.286$, $E_{1/2} = -0.715$ V). The ratio of i_{pa}/i_{pc} was 2.24 V, indicating the quasi-reversible redox process of the metal complex. From the above studies, we suggest that all the metal complexes intercalate into the base pairs of DNA. Electrochemical parameters for the mixed ligand complexes (1-20) on interaction with CT-DNA are shown in Table-5.

Biological studies

Radical-scavenging activity: DPPH is a stable free radical that is often used for detection of the radical-scavenging activity in chemical analysis^{53,54}. Antioxidant properties, radical scavenging activities, are very important due to the deleterious role of free radicals in biological system. The metal complexes used in the study showed good activities as a radical scavenger compared to the scavenging ability of ascorbic acid, which was used as a standard. In the DPPH assay, the ability of the investigated Schiff base ligand(s) and its complexes, to act as donors of hydrogen atoms or electrons in transformation of DPPH radical into its reduced form DPPH-H was investigated. The dissociation energy of the OH bond (L^2) is considered to be one of the most important physicochemical parameters involved in the definition of the antioxidant potency. The ability of the compounds to effectively scavenge DPPH radical is displayed in Fig. 6, where it is compared with that of ascorbic

acid as standard. Lower absorbance values of the reaction mixture indicated higher free radical scavenging activity.

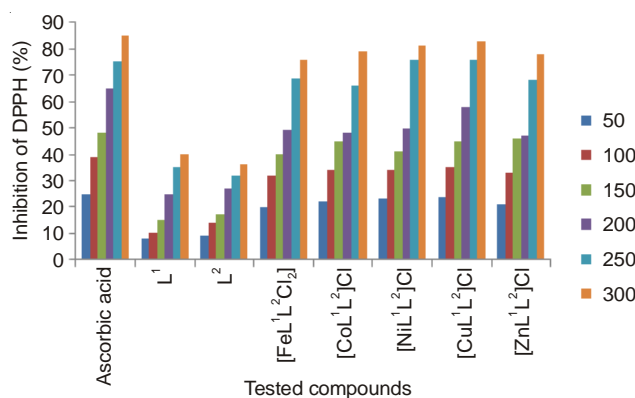


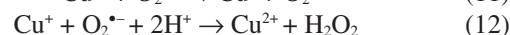
Fig. 6. Antioxidant activity of metal complex

Reducing power: The reducing power of the complexes may serve as a tool for its antioxidant activity. The metal complexes were tested for their relative reducing capacities. The antioxidant activities of putative antioxidants may be attributed to various mechanisms, such as prevention of chain initiation, decomposition of peroxides, prevention of continued hydrogen abstraction and radical scavenging. Thus, in the FRAP (ferric reducing antioxidant power) method, the direct reduction of $Fe^{3+}(CN^-)_6$ to $Fe^{2+}(CN^-)_6$ may be used as a measure of reducing power of mixed ligand complexes. The reducing power of compounds was determined by measuring the absorbance of Perl's Prussian blue complex formed and followed by subsequent reaction with ferric chloride (eqn. ii) to yield the ferric ferrous complex with λ_{max} at 700 nm. The method indicates that greater the absorbance, greater is the antioxidant's reducing capacity for iron⁵⁵ from Fe^{3+} to Fe^{2+} .



In the present work, Cu(II) complex has low reducing power and has high total antioxidant activity than other metal complexes. Since, the reducing power of above complexes was found to be significant in this study. Therefore, this may be considered as potential antioxidants capable of generating Cu(II) ligand radical.

Superoxide dismutase mimic activities: The superoxide dismutase activities of complexes were investigated by NBT assay. Copper gives good superoxide dismutase activity, although its structure is totally unrelated with native enzyme. The ping-pong mechanism of superoxide dismutase activity is given in eqns. (9) and (10).



It has been proposed that electron transfer between Cu(II) and superoxide anion radicals occurs through direct binding. As a consequence of this interaction, these ions undergo rapid reduction to Cu(I) with the release of O_2 molecule. It is assumed that electron transfer between the central metal and $O_2^{\bullet-}$ occurs by direct binding⁵⁶. The fast exchange of axial solvent molecules and a limited steric hindrance to the approach of the $O_2^{\bullet-}$ in that complexes allow a better superoxide dismutase mimic⁵⁷.

TABLE-5
ELECTROCHEMICAL PARAMETERS FOR THE MIXED LIGAND COMPLEXES ON INTERACTION WITH CT DNA

Compound	Redox couple	$E_{1/2}(V)$		$\Delta E_p(V)$		i_{pa}/i_{pc}
		Free	Bound	Free	Bound	
[FeL ¹ L ² Cl ₂] (1)	Fe (III) → Fe(II)	-0.873	-0.861	0.228	0.215	1.21
[CoL ¹ L ²]Cl (2)	Co(II) → Co(I)	-0.817	-0.810	0.194	0.183	1.28
[NiL ¹ L ²]Cl (3)	Ni(II) → Ni(I)	-0.672	-0.665	0.219	0.212	1.41
[CuL ¹ L ²]Cl (4)	Cu(II) → Cu(I)	0.310	0.303	-0.400	-0.396	1.12
	Cu(I) → Cu(0)	-0.923	-0.910	0.355	0.343	1.17
[ZnL ¹ L ²]Cl (5)	Zn(II) → Zn(0)	-0.715	-0.705	0.286	0.275	2.24
[FeL ¹ L ³ Cl ₂] (6)	Fe (III) → Fe(II)	-0.783	-0.771	0.327	0.313	1.35
[CoL ¹ L ³]Cl (7)	Co(II) → Co(I)	-0.738	-0.726	0.268	0.257	1.42
[NiL ¹ L ³]Cl (8)	Ni(II) → Ni(I)	-0.752	-0.764	0.342	0.335	1.11
[CuL ¹ L ³]Cl (9)	Cu(II) → Cu(I)	0.342	0.335	-0.453	-0.442	1.23
	Cu(I) → Cu(0)	-0.895	-0.884	0.286	0.277	1.25
[ZnL ¹ L ³]Cl (10)	Zn(II) → Zn(0)	-0.843	-0.836	0.312	0.305	2.48
[FeL ¹ L ⁴ Cl ₃] (11)	Fe (III) → Fe(II)	-0.739	-0.722	0.253	0.242	1.16
[CoL ¹ L ⁴]Cl (12)	Co(II) → Co(I)	-0.728	-0.705	0.251	0.244	1.48
[NiL ¹ L ⁴]Cl (13)	Ni(II) → Ni(I)	-0.765	-0.751	0.238	0.220	1.19
[CuL ¹ L ⁴]Cl (14)	Cu(II) → Cu(I)	0.328	0.317	-0.427	-0.416	1.13
	Cu(I) → Cu(0)	-0.785	-0.773	0.261	0.255	1.09
[ZnL ¹ L ⁴]Cl (15)	Zn(II) → Zn(0)	-0.765	-0.756	0.242	0.236	2.47
[FeL ¹ L ⁵ Cl ₃] (16)	Fe (III) → Fe(II)	-0.752	-0.743	0.238	0.225	1.75
[CoL ¹ L ⁵]Cl (17)	Co(II) → Co(I)	-0.892	-0.885	0.347	0.335	1.35
[NiL ¹ L ⁵]Cl (18)	Ni(II) → Ni(I)	-0.784	-0.773	0.263	0.257	1.48
[CuL ¹ L ⁵]Cl (19)	Cu(II) → Cu(I)	0.421	0.412	-0.518	-0.512	1.11
	Cu(I) → Cu(0)	-0.923	-0.914	0.259	0.245	1.15
[ZnL ¹ L ⁵]Cl (20)	Zn(II) → Zn(0)	-0.836	-0.824	0.256	0.248	2.49

Fig. 7 represents plot of percentage of inhibiting NBT reduction with an increase in the concentration of complexes. Fig. 8 represents plot of absorbance values against time (t) of Cu(II) complex (4). The percentage of inhibition at various concentrations of the copper complex as a function of time is calculated by measuring the absorbance at 560 nm and the results are plotted to give a straight line. The Cu(II) complexes showed superoxide dismutase-like activity which was evaluated by the scavenger concentration causes 50 % inhibition in the detector formation, IC₅₀. These higher values may be due to the strong field created by the ligands which opposes the interaction of the coordinated Cu(II) with O₂^{•-} radical. The observed results showed that the superoxide scavenging properties and oxidative behaviour of mixed ligand complexes were identical to those of complexes support the above mechanism.

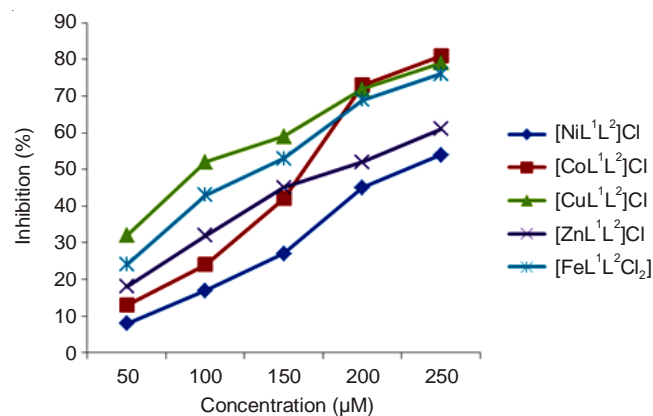


Fig. 7. Plot of percentage of inhibiting NBT reduction with an increase in the concentration of complexes

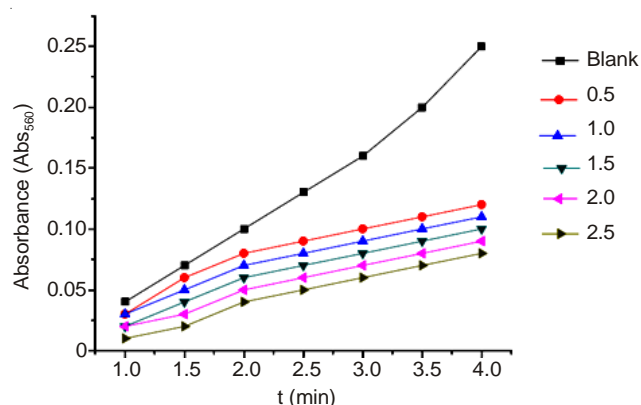


Fig. 8. Plot of absorbance values (Abs₅₆₀) against time (t) in varies concentration of copper complex

Antimicrobial activity: The *in vitro* biological screening effects of the investigated compounds were tested against the bacterial species and fungal species by the disc diffusion method. The minimum inhibitory concentration values of the synthesised compounds were summarized in Tables 6 and 7. A comparative study of the ligands and their metal complexes indicates that complexes exhibit higher antimicrobial activity than the free ligands. The enhanced activity of the complexes can be explained on the basis of overtone's concept⁵⁸ and Tweedy's chelation theory⁵⁹. According to overtone's concept of cell permeability, the lipid membrane that surrounds the cell favors the passage of only the lipid soluble materials makes which liposolubility as an important factor, which controls the antimicrobial activity. On chelation, the polarity of the metal ion will be reduced to a greater extent due to the overlap

TABLE-6
MINIMUM INHIBITORY CONCENTRATION OF THE SYNTHESIZED COMPOUNDS AGAINST GROWTH OF BACTERIA ($\mu\text{g/mL}$)

Comp.	<i>E. coli</i>	<i>K. pneumonia</i>	<i>S. typhi</i>	<i>P. aeruginosa</i>	<i>S. aureus</i>	Comp.	<i>E. coli</i>	<i>K. pneumonia</i>	<i>S. typhi</i>	<i>P. aeruginosa</i>	<i>S. aureus</i>
L ¹	54	57	63	55	60	[FeL ¹ L ⁴ Cl ₃] (11)	37	28	39	31	27
L ²	57	57	66	52	63	[CoL ¹ L ⁴ Cl]Cl (12)	33	25	37	26	23
L ³	58	59	68	56	61	[NiL ¹ L ⁴ Cl]Cl (13)	33	25	34	25	20
L ⁴	56	58	65	56	63	[CuL ¹ L ⁴ Cl]Cl (14)	21	23	28	23	17
L ⁵	58	61	69	57	67	[ZnL ¹ L ⁴ Cl]Cl (15)	35	26	32	29	26
[FeL ¹ L ² Cl ₂] (1)	37	28	38	31	29	[FeL ¹ L ⁵ Cl ₃] (16)	39	31	37	35	29
[CoL ¹ L ²]Cl (2)	32	26	34	25	25	[CoL ¹ L ⁵ Cl]Cl (17)	35	26	35	27	25
[NiL ¹ L ²]Cl (3)	31	24	32	24	23	[NiL ¹ L ³ Cl]Cl (18)	32	23	34	29	23
[CuL ¹ L ²]Cl (4)	22	25	31	21	15	[CuL ¹ L ⁵ Cl]Cl (19)	25	27	21	29	14
[ZnL ¹ L ²]Cl (5)	33	27	37	28	27	[ZnL ¹ L ⁵ Cl]Cl (20)	37	28	35	32	31
[FeL ¹ L ³ Cl ₂] (6)	39	28	37	32	27	Pencillin	12	10	8	2	6
[CoL ¹ L ³]Cl (7)	33	23	32	29	21	Ampicillin	10	8	9	6	3
[NiL ¹ L ³]Cl (8)	28	25	30	28	19	Vancomycin	8	12	3	7	13
[CuL ¹ L ³]Cl (9)	26	23	29	26	15	Ofloxacin	5	13	4	6	11
[ZnL ¹ L ³]Cl (10)	36	26	36	29	20	—	—	—	—	—	—

TABLE-7
MINIMUM INHIBITORY CONCENTRATION OF THE SYNTHESIZED COMPOUNDS AGAINST GROWTH OF FUNGI ($\mu\text{g/mL}$)

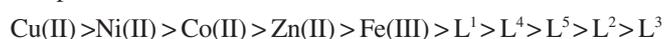
Comp.	<i>A. niger</i>	<i>R. stolonifer</i>	<i>A. flavus</i>	<i>R. bataicola</i>	<i>C. albicans</i>	Comp.	<i>A. niger</i>	<i>R. stolonifer</i>	<i>A. flavus</i>	<i>R. bataicola</i>	<i>C. albicans</i>
L ¹	56	50	64	64	50	[ZnL ¹ L ³]Cl (10)	27	30	34	33	35
L ²	58	52	63	65	57	[FeL ¹ L ⁴ Cl ₃] (11)	27	29	37	34	25
L ³	61	53	66	70	63	[CoL ¹ L ⁴ Cl]Cl (12)	23	27	34	35	27
L ⁴	55	56	68	63	57	[NiL ¹ L ⁴ Cl]Cl (13)	17	25	28	32	24
L ⁵	62	55	64	72	69	[CuL ¹ L ⁴ Cl]Cl (14)	15	22	25	29	21
[FeL ¹ L ² Cl ₂] (1)	30	29	40	37	27	[ZnL ¹ L ⁴ Cl]Cl (15)	25	28	33	37	30
[CoL ¹ L ²]Cl (2)	23	25	35	33	29	[FeL ¹ L ⁵ Cl ₃] (16)	28	32	36	36	34
[NiL ¹ L ²]Cl (3)	19	27	30	35	26	[CoL ¹ L ⁵ Cl]Cl (17)	25	29	32	34	30
[CuL ¹ L ²]Cl (4)	17	25	28	32	21	[NiL ¹ L ⁵ Cl]Cl (18)	19	28	29	35	28
[ZnL ¹ L ²]Cl (5)	25	29	36	37	30	[CuL ¹ L ⁵ Cl]Cl (19)	17	26	27	30	25
[FeL ¹ L ³ Cl ₂] (6)	32	33	36	40	31	[ZnL ¹ L ⁵ Cl]Cl (20)	26	30	35	37	34
[CoL ¹ L ³]Cl (7)	25	31	35	38	29	Nystatin	12	14	6	17	12
[NiL ¹ L ³]Cl (8)	22	30	32	36	26	Ketoconazole	11	9	15	15	13
[CuL ¹ L ³]Cl (9)	19	28	30	34	25	Clotrimazole	8	10	13	12	11

of the ligand orbital and partial sharing of the positive charge of the metal ion with donor groups. Further, it increases the delocalization of π -electrons over the whole chelate ring and enhances the lipophilicity of the complexes.

Metal chelates bear polar and nonpolar properties together; this makes them suitable for permeation to the cells and tissues. In addition, chelation may enhance or suppress the biochemical potential of bioactive organic species. Changing hydrophilicity and lipophilicity probably leads to bring down the solubility and permeability barriers of cell. Further, lipophilicity, which controls the rate of entry of molecules into the cell, is modified by coordination, so the metal complex can become more active than the free ligand⁶⁰. However, compared to the antimicrobial activity of the standards, the activity exhibited by the ligand and the metal complexes was lower.

This increased lipophilicity enhances the permeation of the complexes into lipid membranes and blocking of the metal binding sites in the enzymes of microorganisms. These complexes also disturb the respiration process of the cell and thus block the synthesis of the proteins that restricts further growth of the organism and as a result microorganisms die. The increased activity of the complexes may also be explained on the basis of their high solubility, fitness of the particles, size of

the metal ion and the presence of the bulkier organic moieties. The different lipophilic behaviour of the aromatic residues such as antipyrine and furfuraldehyde is involved in the biological activity mechanisms. The activity order of the synthesized compounds is as follows:



The reason for high antimicrobial activity of copper complex can be explained in terms of the effect of copper metal ion on the normal cell process. The complexation reaction reduces the polarity of the metal ion by the partial sharing of metal ion positive charge with donor groups and electron delocalization over the chelate ring⁶¹. Thus, the lipophilic character of the central metal atom is enhanced which results in a higher capability to penetrate the microorganisms through the lipid layer of the cell membrane.

Conclusion

A series of mixed ligand complexes with 4-aminoantipyrine were synthesized and characterized by elemental analysis, spectral techniques. From the DNA binding studies indicates that the complexes have intercalative binding mode. Antimicrobial activity studies show that the complexes showed better biological activity as compared to free ligand. The

synthesized complexes exhibit significant superoxide dismutase mimetic and reducing power activities. In our present work would be very useful in the development of potential applications in biological, pharmaceutical and physiological fields in future.

REFERENCES

1. A.A. Khandar, S.A. Hosseini-Yazdi, S.A. Zarei and U.M. Rabie, *Inorg. Chim. Acta*, **358**, 3211 (2005).
2. W.U. Malik and R. Jain, *J. Indian Chem. Soc.*, **54**, 558 (1982).
3. T.D. Bradshaw, M.C. Bibby, J.A. Double, I. Fichtner, P.A. Cooper, M.C. Alley, S. Donohue, S.F. Stinson, J.E. Tomaszewski, E.A. Sausville and M.F. G. Stevens, *Mol. Cancer Ther.*, **1**, 239 (2002).
4. E. Sidoova, D. Loos, H. Bujdakova and J. Kallová, *Molecules*, **2**, 36 (1997).
5. B. Alain, D.M. Christinonie I. Assunta and C.A. Patent, *Pharmaceuticals*, **1**, 63 (1997).
6. E. Abignente, P. De-Capariis, A. Sacchi and E. Marmole, *Farmaco Sci.*, **38**, 533 (1983).
7. C. Ramalingan, S. Balasubramanian, S. Kabilan and M. Vasudevan, *Eur. J. Med. Chem.*, **39**, 527 (2004).
8. G. Turan-Zitouni, S. Demirayak, A. Özdemir, Z.A. Kaplancikil and M.T. Yıldız, *Eur. J. Med. Chem.*, **39**, 267 (2004).
9. M.A. Neelakantan, S.S. Marriappan, J. Dharmaraja, T. Jeyakumar and K. Muthukumar, *Spectrochim. Acta A*, **71**, 628 (2008).
10. G.H. Alt, US Patent 4,226, 615 (1980); *Chem. Abstr.*, **94**, 26155 (1981).
11. Y. Hamada, I. Takeuchi, Y. Ita, S. Matsui and T. Ita, *Yakugaku Zasshi*, **101**, 633 (1981); *Chem. Abstr.*, **95**, 181559 (1981).
12. M. Ismail, *Indian J. Pharm. Sci.*, **45**, 121 (1986); *Chem. Abstr.*, **107**, 175589 (1987).
13. P.O. Lumme and H. Knuutila, *Polyhedron*, **14**, 1553 (1995).
14. R.A. Holley and D. Patel, *Food Microbiol.*, **22**, 273 (2005).
15. (a) M.A.R. Amalaradjou, S.A. Baskaran, R. Ramanathan, A.K. Johnny, A.S. Charles, S.R. Valipe, T. Mattson, D. Schreiber, V.K. Juneja, R. Mancini and K. Venkitanarayanan, *Food Microbiol.*, **27**, 841 (2010); (b) R. Becerril, R. Gomez-Lus, P. Goni, P. Lopez and C. Nerin, *Anal. Bioanal. Chem.*, **388**, 1003 (2007); (c) L. Guillier, A.I. Nazer and F. Dubois-Brissonnet, *J. Food Prot.*, **70**, 2243 (2007).
16. J.M. Dornish, E.O. Pettersen and R. Oftebro, *Cancer Res.*, **49**, 3917 (1989).
17. S. Cunha, S.M. Oliveira, M.T. Rodrigues Jr., R.M. Bastos, J. Ferrari, C.M.A. de Oliveira, L. Kato, H.B. Napolitano, I. Vencato and C. Lariucci, *J. Mol. Struct.*, **752**, 32 (2005).
18. S.A.J. Coolen, F.M. Everaerts and F.A. Huf, *J. Chromatogr. A*, **788**, 95 (1997).
19. M.E. Wolff, *Burger's Medicinal Chemistry*, edn 3, Wiley: New York, USA, Vol. 1, pp. 393-418 (1970).
20. A.G. Gilman, L.S. Goodman and A. Gilman, *The Pharmacological Basis of Therapeutics*, Macmillan Publishing Co: New York, USA, pp. 391-447 (1980).
21. T. Rosu, S. Pasculescu, V. Lazar, C. Chifiriuc and R. Cernat, *Molecules*, **11**, 904 (2006).
22. V.C. Filho, R. Correa, Z. Vaz, J.B. Calixto, R.J. Nunes, T.R. Pinheiro, A.D. Andricopulo and R.A. Yunes, *Farmaco*, **53**, 55 (1998).
23. G. Turan-Zitouni, M. Sivaci, F.S. Kilic and K. Erol, *Eur. J. Med. Chem.*, **36**, 685 (2001).
24. O.I. Singh, M. Damayanti, N.R. Singh, R.K.H. Singh, M. Mohapatra and R.M. Kadam, *Polyhedron*, **24**, 909 (2005).
25. E.K. Efthimiadou, M.E. Katsarou, A. Karaliota and G. Psomas, *J. Inorg. Biochem.*, **102**, 910 (2008).
26. J.M. McCord, *Enzymol.*, **349**, 331 (2002).
27. C.C. Winterbourn, *Free Radic. Biol. Med.*, **14**, 85 (1993).
28. I. Fridovich, *Annu. Rev. Biochem.*, **64**, 97 (1995).
29. A.F. Miller, *Curr. Opin. Chem. Biol.*, **8**, 162 (2004).
30. A.I. Vogel, *A Textbook of Quantitative Inorganic Analysis Including Elementary Instrumental Analysis* edn 4, Longman, London (1978).
31. M.E. Bodini, M. Angelica del Valle and S. Cáceres, *Polyhedron*, **16**, 2903 (1997).
32. R.L. De, M. Mandal, L. Roy, J. Mukherjee and B.K.M. Ruchika, *Indian J. Chem.*, **47A**, 1480 (2008).
33. V.D. Bhatt and S.R. Ram, *J. Chem. Sci.*, **63**, 1 (2012).
34. Y. Chen, M. Wang, R.T. Rosen and C.T. Ho, *J. Agric. Food Chem.*, **47**, 2226 (1999).
35. R.G. Bhirud and T.S. Srivastava, *Inorg. Chim. Acta*, **179**, 125 (1991).
36. W.J. Geary, *Coord. Chem. Rev.*, **7**, 81 (1971).
37. A.B.P. Lever, *Inorganic Electronic Spectroscopy* edn 2, New York: Elsevier (1968).
38. A.B.P. Lever and E. Mantovani, *Inorg. Chem.*, **10**, 817 (1971).
39. A.B.P. Lever, *Inorganic Electronic Spectroscopy*, edn 2, Elsevier, New York (1968).
40. G. Maki, *J. Chem. Phys.*, **28**, 651 (1958).
41. H. Temel, S. İlhan, M. Sekerci and R. Ziyadanogullari, *Spectrosc. Lett.*, **35**, 219 (2002).
42. B.J. Hathaway and D.E. Billing, *Coord. Chem. Rev.*, **5**, 143 (1970).
43. R.K. Ray and G.R. Kauffman, *Inorg. Chim. Acta*, **173**, 207 (1990).
44. R. Pogni, M.C. Baratto, A. Diaz and R. Basosi, *J. Inorg. Biochem.*, **79**, 333 (2000).
45. J.B. Le Pecq and C. Paoletti, *J. Mol. Biol.*, **27**, 87 (1967).
46. S. Satyanarayana, J.C. Dabrowiak and J.B. Chaires, *Biochemistry*, **32**, 2573 (1993).
47. Y. Xiong, X.F. He, X.H. Zou, J.Z. Wu, X.M. Chen, L.N. Ji, R.H. Li, J.Y. Zhou and K.B. Yu, *J. Chem. Soc., Dalton Trans. I*, 19 (1999).
48. G.L. Zubry, *Biochemistry*, MacMillan, New York, edn 2, p. 236 (1988).
49. J. SantaLucia, *Proc. Natl. Acad. Sci. USA*, **95**, 1460 (1998).
50. S. Arounaguiri and B.G. Maiya, *Inorg. Chem.*, **35**, 4267 (1996).
51. A. McCoubrey, H.C. Latham, P.R. Cook, A. Rodger and G. Lowe, *FEBS Lett.*, **73**, 380 (1996).
52. E. Tselepi-Kalouli and N. Katsaros, *J. Inorg. Biochem.*, **37**, 271 (1989).
53. J.R. Soare, T.C.P. Dinis, A.P. Cunha and L. Almeida, *Free Radic. Res.*, **26**, 469 (1997).
54. P.D. Duh, Y.Y. Tu and G.C. Yen, *Lebensm.-Wissen. Technol.*, **32**, 269 (1999).
55. I. Gulcin, F. Topal, S.B.O. Sarikaya, E. Bursal, G. Bilsel and A.C. Goren, *Rec. Nat. Prod.*, **5**, 158 (2011).
56. J. Gabrielska, M. Soczynska-Kordala, J. Hladyszowski, R. Zylka, J. Miskiewicz and S. Przystalski, *J. Agric. Food Chem.*, **54**, 7735 (2006).
57. J.A. Fee, in ed.: H. Sigel, *Metal Ions in Biological System*, vol. 28, Marcel Dekker, New York, pp. 455-505 (1981).
58. S. Belaid, A. Landreau, S. Djebbar, O. Benali-Baitich, G. Bouet and J.-P. Bouchara, *J. Inorg. Biochem.*, **102**, 63 (2008).
59. N. Dharmaraj, P. Viswanathamurthi and K. Natarajan, *Transition Met. Chem.*, **26**, 105 (2001).
60. N. Farrell, *Coord. Chem. Rev.*, **232**, 1 (2002).
61. H. Arslan, N. Duran, G. Borekci, C. Koray Ozer and C. Akbay, *Molecules*, **14**, 519 (2009).